

Warning Signs for Wave Speed Transitions of Noisy Fisher-KPP Invasion Fronts

Christian Kuehn

the date of receipt and acceptance should be inserted later

Abstract Invasion waves are a fundamental building block of theoretical ecology. In this study we aim to take the first steps to link propagation failure and fast acceleration of traveling waves to critical transitions (or tipping points). The approach is based upon a detailed numerical study of various versions of the Fisher-Kolmogorov-Petrovskii-Piscounov (FKPP) equation. The main motivation of this work is to contribute to the following question: how much information do statistics, collected by a stationary observer, contain about the speed and bifurcations of traveling waves? We suggest warning signs based upon closeness to carrying capacity, second-order moments and transients of localized initial invasions.

Keywords: Critical transitions, invasion waves, propagation failure, Fisher-KPP, FKPP, SPDE.

1 Introduction

The propagation of waves has been a central topic in spatial ecology for a long time. A primary motivation arises from fronts where a new species is introduced into an environment or an existing species considerably extends its habit. A classical example is the spread of muskrats in central Europe [77]. Other documented examples are butterflies and bush crickets in the UK [79] and the cane toad invasion in Aus-

tralia [63]. Also bacterial growth [54, 26] shows very similar spreading and wave phenomena. The references in [31, 76] contain even more examples.

From a theoretical perspective a first groundbreaking result is the modelling of invasion waves via reaction-diffusion equations by [22] and Kolmogorov, Petrovskii, Piscounov [43] (FKPP) who studied the partial differential equation (PDE)

$$\frac{\partial u}{\partial t} = \frac{\partial^2 u}{\partial x^2} + u(1 - u). \quad (1)$$

There are many different aspects that could be included in a reaction-diffusion model which are very interesting to match theory and experiment; see [31, 33, 20, 53]. Nevertheless, the basic guiding principles obtained from simple models are still highly relevant. Here we shall restrict ourselves to the study of the following stochastic partial differential equation (SPDE)

$$\frac{\partial u}{\partial t} = \frac{\partial^2 u}{\partial x^2} + f(u) + \text{'noise'}. \quad (2)$$

For now, the reader may just think of the classical FKPP nonlinearity $f(u) = u(1 - u)$ and some noise process that vanishes at zero-population level; for more technical details see Sections 3-4. The detailed choices are discussed later.

The main theme of this paper is the interplay between invasion waves and so-called critical transitions [71, 45]. Basically, critical transitions (or tipping points) are drastic sudden changes in dynamical systems; for some background and details see Section 2. The first major question is whether (1)-(2) can undergo a 'critical transition'. We discuss this question from a more technical perspective in Section 2. On a

C. Kuehn
Vienna University of Technology,
Institute for Analysis and Scientific Computing,
Vienna, 1040, Austria.
E-mail: ck274@cornell.edu

heuristic level, one may just consider a parameter in (2) that is slowly varying. Suppose that there exists a wave with positive speed for some parameter range while the wave is stationary (or reverses direction) for another parameter range. Whether an invasion reaches a new habitat or not can have drastically different consequences so one probably would like to refer to this situation as a critical transition.

Another case we shall consider in this paper is the situation where the wave speed becomes infinite at a special parameter value. Hence, a small parameter variation can cause a dramatically accelerating invasion wave.

The next step is to check whether early-warning signs for a critical transition exist. In this context, changes in vegetation patterns have been the main motivation recently [41,34]. There are only a few studies on early-warning signs for spatial systems [14,13]. In fact, early-warning signs for noisy waves generated by SPDEs have not been considered yet. This paper makes a first step in this direction. We focus on transitions for the wave speed (e.g. propagation failure) as it controls when and where an invasion front appears. Although some detailed measurements of waves are available [35,51] it is very difficult to obtain precise global empirical information [31, p.92] about a wave. Here we restrict ourselves to a single spatial observation location i.e. records by a single stationary 'ecological observer' over a fixed time interval. The general idea that one may obtain spatial conclusions from local observations is not new [21]. However, our detailed comparative numerical study of several different variants of (2) with a focus on local early-warning signs seems to be a completely new direction; for more details on the numerical methods see Section 5. The main themes and results from the numerical studies are the following:

- (a) A description of the statistics for early-warning signs in SPDEs with wave propagation failure based upon closeness to carrying capacity and second-order moments.
- (b) A comparative study of (a) for different noise types (white, space-time white) and different multiplicative noise nonlinearities (parametric, finite-system size, etc.).
- (c) Investigation of statistics near continuous wave speed transitions (and their unpredictability) for Allee effect nonlinearities in the deterministic part of the FKPP SPDE.
- (d) Suggestion of transient minima to analyze wave propagation failure and wave speed blow-up.

Beyond the technical contributions we also try to link different methodologies. We combine approaches from biological invasions, critical transitions, Fisher-KPP (and Nagumo) waves, SPDEs and numerical methods. This approach should also be helpful to link several, mostly distinct, communities such as theoretical ecology, waves in theoretical physics and mathematical methods for SPDEs.

The paper is organized as follows. In Sections 2-5 we give brief reviews of the essential facts required for the remaining part of the paper. Due to the interdisciplinary aspects, the brief reviews seem necessary. Readers familiar with all the background may forward to Section 6 where the multiplicative noise case for the FKPP SPDE and statistical warning signs are studied. The nonlinear noise case is considered in Section 7 and the Allee effect in Section 8. Section 9 on transient phenomena and the influence of initial conditions concludes the main part of the paper. In Section 10 a number of generalizations and open problems are listed.

2 Background - Critical Transitions

A primary motivation to study critical transitions (or tipping points) arose from ecology, e.g. due to the theoretical work of Scheffer and co-workers [73, 72, 74]. Then it became clear from many distinct applied problems [71] as well as from abstract mathematical considerations [45, 46] that many features for early-warning signs are generic across many dynamical systems. Recent studies of laboratory [16, 82] and full ecosystem [9] experiments re-inforced this viewpoint.

Here we recall a few aspects of critical transitions for finite-dimensional systems relevant for this paper. Consider the pitchfork bifurcation normal form [47, p.282]

$$\frac{dw}{dt} = w' = \mu w + w^3, \quad \text{for } w \in \mathbb{R}, \mu \in \mathbb{R}. \quad (3)$$

The homogeneous trivial branch $\{w = 0\}$ consists of stable equilibria for $\mu < 0$ and unstable equilibria for $\mu > 0$ since the linearized system around $w = 0$ is $W' = \mu W$ with solution $W(t) = W(0)e^{\mu t}$. The bifurcation at $\mu = 0$ is sub-critical with two unstable branches $\{w = \pm\sqrt{-\mu}\}$ for $\mu < 0$.

Consider a slow parameter variation $\mu' = \epsilon$ with $0 < \epsilon \ll 1$ and $\mu(0) < 0$. Orbits near the homogeneous branch will reach a neighborhood of $(w, \mu) =$

$(0, 0)$ and then jump away quickly indicating a critical transition [45, Fig.3(c)]. Before the jump the system is slow to recover from perturbations ('slowing down') for $\mu < 0$ since $W(0)e^{\mu t} \rightarrow W(0)$ as $\mu \rightarrow 0$ for fixed t . For a deterministic system, it is impossible to measure the slowing-down effect once it starts tracking the homogeneous branch $\{w = 0\}$ i.e. it is exponentially close to $w = 0$. However, for a stochastic version of (3) given by

$$w' = \mu w + w^3 + \text{'noise'} \quad (4)$$

the random perturbations can constantly kick the system away from the trivial branch. Extracting statistics from these perturbations can make the slowing down effect measurable [71, 45]. This is one motivation to study stochastic traveling waves (2).

An important question is which bifurcation points or quantitative transitions we would like to classify as critical transitions. In multiple time scale systems, such as (4) augmented with $\mu' = \epsilon$, the classification of local bifurcation points is relatively straightforward [46, Sec.2-3]. The mathematical classification and early-warning signs from [45, 46] can be applied to many pattern-forming bifurcations in spatially extended systems on bounded domains. One first derives the amplitude equations on the domain locally [12]. Only a discrete set of eigenvalues occurs [36, p.210] and the usual local bifurcations for a finite number of eigenvalues passing through the imaginary axis can often be applied.

For patterns on unbounded domains the situation is less clear. We do not offer any solution to this problem and consider an example to illustrate the difficulties. Consider a traveling wave solution $u(x, t) = u(x - ct)$, e.g. for (1), with $(x, t) \in \mathbb{R} \times \mathbb{R}^+$ which satisfies $u(x, 0) = 1$ for $x \leq 0$ and $u(x, 0) = 0$ for $x > 0$. Imagine a habitat $[x_1, x_2] \subset \mathbb{R}$ with $x_{1,2} > 0$ and define the mapping

$$\mathcal{I}(u, T) = \frac{1}{|x_2 - x_1|} \int_{x_1}^{x_2} |u(x, T)| dx.$$

If the invasion wave spreads towards $x = \infty$ ($s > 0$) and saturates at the carrying capacity $u \equiv 1$ then there exists a finite time T_i such that for all $T \geq T_i$ we have $\mathcal{I}(u, T) = 1$. If a slow parameter variation causes the wave to become stationary ($s = 0$) then $\mathcal{I}(u, T) = 0$ for all $T \geq 0$. Although this indicates how one may define one possible critical transition scenario for waves, the situation is actually unclear since for fixed $T > 0$ one may have $\mathcal{I}(u, T) = 0$ for

$s > 0$ and $s = 0$. This illustrates again that global definitions are intricate [46, Sec.8].

For this paper we simply rely on the intuitive notion that the transition to a standing wave and also the transition to wave speed blow-up are important in the context of critical transitions and early-warning signs.

3 Background - FKPP Equation(s)

A more general version of the PDE (1) studied by Fisher [22] as well as by Kolmogorov, Petrovskii and Piscounov [43] is given by

$$\frac{\partial u}{\partial t} = D \frac{\partial^2 u}{\partial x^2} + f(u; \mu) \quad (5)$$

for $u = u(x, t)$, $(x, t) \in \mathbb{R} \times [0, \infty)$. The parameter $D > 0$ controls the diffusion and if $f(u; \mu) = \mu f(u)$ then $\mu > 0$ can be interpreted as a growth rate. Of course, an initial condition has to be specified. Often one considers $u(x, t = 0)$ either with compact support localized near $x = 0$ or an initial condition with Gaussian decay. The localized initial condition for a population u to appear in a new environment is not only a mathematical simplification but does occur under realistic conditions e.g. due to global long-range transportation networks [44].

The nonlinearity $f : \mathbb{R}^2 \rightarrow \mathbb{R}$ represents growth and saturation effects and is required to satisfy the conditions

$$\begin{aligned} f(0; \mu) &= 0, & f'(0; \mu) &> 0, \\ f(1; \mu) &= 0, & f'(1; \mu) &< 0. \end{aligned}$$

The classical example is logistic growth $f(u; \mu) = \mu u(1 - u)$. In this case one may rescale $t \mapsto t/\mu$, $x \mapsto x\sqrt{D/\mu}$ to obtain from (5) the FKPP equation

$$\frac{\partial u}{\partial t} = \frac{\partial^2 u}{\partial x^2} + u(1 - u). \quad (6)$$

Initially, the FKPP equation (6) modeled the spread of genes in a population but it has since become a paradigmatic model for populations dispersing under the influence of diffusion [59, p.439-444]. Using a traveling wave ansatz $u(x, t) = u(x - ct) =: u(\xi)$ for (6) yields the ODE

$$\frac{d^2 u}{d\xi^2} + c \frac{du}{d\xi} + u(1 - u) = 0. \quad (7)$$

Analyzing (7) in the phase space variables $(u, u') =: (u, v)$ shows that the point $(u, v) = (1, 0)$ is a saddle and $(u, v) = (0, 0)$ is a stable node or spiral. It is

straightforward [59, p.441-442] to check that heteroclinic orbits from $(1, 0)$ to $(0, 0)$ with $u \geq 0$, which correspond to non-negative traveling waves, can only exist in the stable node case for wave speeds $c \geq 2$. Since the orbit is directed from $u = 1$ to $u = 0$ one also refers to this situation as the stable state $u \equiv 1$ invading the unstable state $u \equiv 0$; see Figure 1(a).

Remark: Wave speeds $c > 0$ correspond to waves traveling to the right. However, the FKPP equation (6) is invariant under the symmetry $x \rightarrow -x$ so that a localized initial condition near $x = 0$ triggers a pair of fronts, one traveling to the left one to the right.

It is known that the traveling wave solutions to (6) form the important solution set [30, Thm 1.4-1.5]. The minimal wave speed $c_{FKPP}^* = 2$ is the asymptotic speed of propagation for the FKPP non-linearity [4]. Since the wave speed is determined by the linearized problem

$$\frac{\partial \tilde{u}}{\partial t} = \frac{\partial^2 \tilde{u}}{\partial x^2} + \tilde{u} \quad (8)$$

at the leading edge near $(u, v) = (0, 0)$ as detailed in [81, p.38-42] one also refers to the traveling wave with $c_{FKPP}^* = 2$ as a pulled front. For a more general nonlinearity $f(u; \mu)$ pushed fronts can exist where the asymptotic wave speed c is larger than the linear spreading speed c^* [81, p.56]. The wave speed for both types is asymptotic and only achieved after a transient period. For pulled fronts the asymptotic expansion yields [81, p.78]

$$c(t) = c^* - \frac{k_1}{t} + \frac{k_2}{t^{3/2}} + \mathcal{O}\left(\frac{1}{t^2}\right), \quad \text{as } t \rightarrow \infty$$

with explicitly computable positive constants $k_{1,2} > 0$. Hence, the wave speed is approached from below by a power law for pulled fronts. For pushed fronts the convergence to the asymptotic speed is exponentially fast [81, p.74]. Another correction occurs when a cutoff for the reaction term is introduced [7] which leads to a logarithmic correction term. Furthermore, if an initial condition does not decay fast enough as $|x| \rightarrow \infty$ then faster speeds than c^* occur [81, p.46]. In particular, for an initial condition decaying like $\mathcal{O}(e^{-\alpha|x|})$ for $\alpha > 0$ the speed increases as $c(\alpha) = \mathcal{O}(1/\alpha)$ as $\alpha \rightarrow 0$ [70].

The results for invasion fronts of the FKPP equation already indicate that the variety of scaling behaviors could be ideal to determine early-warnings. In fact, wave spreading in the stochastic case is even more intricate [48, 49].

4 Background - Stochastic PDEs

As a stochastic generalization of (5) the intuitive idea is to consider the equation

$$\frac{\partial u}{\partial t} = D \frac{\partial^2 u}{\partial x^2} + \mu f(u) + g(u)\eta(x, t) \quad (9)$$

where $\eta(x, t)$ formally represents the 'noise'. Here we consider two choices for the term $\eta(x, t)$. The simplest is to consider a real-valued (1D) Brownian motion $B(t)$ [17, Chapter 8] with mean $\mathbb{E}[B(t)] = 0$ and covariance $\mathbb{E}[B(t)B(s)] = \min(t, s)$ for $0 \leq s \leq t$. Then white noise can be defined via $\eta(x, t) = \dot{B}$ where the derivative is with respect to time and interpreted in the generalized sense [3, p.52-53]. The covariance is $\mathbb{E}[\eta(t)\eta(s)] = \delta(t-s)$ and one may then write (9) in two equivalent forms

$$\begin{aligned} \frac{\partial u}{\partial t} &= D \frac{\partial^2 u}{\partial x^2} + \mu f(u) + g(u)\dot{B}(t), \\ du &= \left[D \frac{\partial^2 u}{\partial x^2} + \mu f(u) \right] dt + g(u)dB. \end{aligned} \quad (10)$$

The existence and regularity theory of (10) is well understood [23]. If the noise should depend on space and time the theory is substantially more involved.

One possibility is to consider a Hilbert space U (e.g. $L^2(\mathbb{R})$) and a symmetric non-negative linear operator Q acting on U and define a U -valued Q -Wiener process $W(t)$. If $Tr(Q) < +\infty$ there exists a complete orthonormal system $\{f_k\}_{k=1}^\infty$ such that

$$Qf_k = \lambda_k f_k, \quad \text{for } k \in \mathbb{N}$$

where $\{\lambda_k\}_{k=1}^\infty$ is a nonnegative bounded sequence. Then one may use the convergent sequence

$$W(t) = \sum_{k=1}^{\infty} \sqrt{\lambda_k} B_k(t) f_k \quad (11)$$

with independent one-dimensional Brownian motions $B_k(t)$ as a definition [66, p.86-89]. As expected one has $\mathbb{E}[W(t)] = 0$ and $\mathbb{E}[W(t)W(s)] = \min(t, s)Q$ so that Q can be viewed as the covariance operator. In this case one may formally write (9) as looking for $u = u(\cdot, t)$ in the form

$$\begin{aligned} \frac{\partial u}{\partial t} &= D \frac{\partial^2 u}{\partial x^2} + \mu f(u) + g(u)\dot{W} \\ du &= \left[D \frac{\partial^2 u}{\partial x^2} + \mu f(u) \right] dt + g(u)dW. \end{aligned} \quad (12)$$

which can be interpreted in a precise integral form [66, Section 5.1]. A well-developed existence theory for (12) is available [66, Thm 7.4, Thm 7.6].

One is tempted to take $Q = Id$ to mirror the finite-dimensional case to obtain a 'white noise' process. However, $Q = Id$ is not of trace-class (since

$Tr(Q) = +\infty$) and the series (11) does not converge. However, one may construct a cylindrical Wiener process for $Q = Id$ [66, p.96-99] and characterize space-time white noise as $\dot{W} = \eta(x, t)$ which has covariance $\mathbb{E}[\eta(x, t)\eta(y, s)] = \delta(x - y)\delta(t - s)$. The existence and regularity theory for space-time white noise is slightly more involved and already leads to problems if $x \in \mathbb{R}^2$ [10, p.54]. Since we exclusively restrict to $x \in \mathbb{R}$ these problems do not arise here and the existence theory works [29, Section 6.1].

Remark: Instead of viewing the equation on function spaces one may also consider an approach [84] where the solution $u = u(x, t)$ is a real-valued random field which is a basically equivalent [39] approach. In this case, one has $\mathbb{E}[W(x, t)W(y, s)] = \min(t, s) \min(x, y)$ and that space-time white noise is $\frac{\partial^2}{\partial x \partial t} W(x, t) = \eta(x, t)$.

5 Background - Numerical SPDEs

First, we briefly review basic methods to solve the SPDE (12) numerically for space-time white noise. The case (10) will follow as a special case. A natural first step is to start with a spatial discretization [37]. Consider a finite interval $[x_1, x_N] \subset \mathbb{R}$ for some $N > 1$ and augment (12) with zero, reflective or periodic boundary conditions. Define $(\Delta x) := (x_N - x_1)/N$ and consider the numerical solution $U_j(t) \approx u(x_1 + (j - 1)(\Delta x), t)$. Then the space-discrete version of (12) is a system of stochastic ordinary differential equations (SODEs)

$$dU_j = \underbrace{\left[\frac{D}{(\Delta x)^2} \sum_{l=1}^N L_{jl} U_l + \mu f(U_j) \right]}_{=: F_j(U)} dt + \underbrace{\frac{g(U_j)}{\sqrt{\Delta x}}}_{G_{jj}(U)} dB_j, \quad (13)$$

for $j = 1, 2, \dots, N$ where $\{B_j\}_{k=1}^N$ are independent one-dimensional Brownian motions and the $N \times N$ matrix L depends on the boundary conditions. For reflection conditions [24] it follows that $L_{jj} = -2$ if $j \in \{2, 3, \dots, N - 1\}$, $L_{11} = -1 = L_{NN}$, $L_{ij} = 1$ if $|i - j| = 1$ and $L_{ij} = 0$ otherwise. For periodic conditions [24] one uses $L_{jj} = -2$ for all j , $L_{1N} = 1 = L_{N1}$, $L_{ij} = 1$ if $|i - j| = 1$ and $L_{ij} = 0$ otherwise. For zero boundary conditions [28] the values $u_1^N \equiv 0 \equiv u_N^N$ are fixed, the first and last equation in (13) are discarded and the $(N - 2) \times (N - 2)$ matrix L

obeys $L_{jj} = -2$ for $j \in \{2, 3, \dots, N - 1\}$, $L_{ij} = 1$ if $|i - j| = 1$ and $L_{ij} = 0$ otherwise. For the simpler case (10) one has a single Brownian motion so that $B_j = B$ for all j and the factor $1/\sqrt{\Delta x}$ in (13) is removed [24].

It remains to solve the SODE (13) which can be more compactly written as

$$dU = F(U)dt + G(U)dB \quad (14)$$

where we view $F(U) = (F_1(U), \dots, F_N(U))^T$, $B = (dB_1, \dots, dB_N)^T$ as (column) vectors and $G(U)$ is a diagonal matrix with diagonal entries $G_{jj}(U)$. As a numerical scheme we shall always use either use the Euler-Maruyama method [32] or the the Milstein method in its explicit [42, p.345-351] or implicit [42, p.399-404] form stated below.

Remark: The Milstein method is usually good as an exploratory tool due to its robustness. It has strong order-one convergence [42, Thm 10.3.5]. It is relatively straightforward to implement the Milstein method as no multiple stochastic integral evaluations occur since $x \in \mathbb{R}$ [42, Chapter 10-11][38, p.2]. Furthermore, it has recently been shown that it nicely extends to multiplicative trace-class noise [38]. Hence, the Milstein method provides a quite remarkable compromise between theoretical error estimates and practical implementation issues; see also [32] for a computational introduction with test codes for scalar problems. The Euler-Maruyama method is faster but not as robust so it complements Milstein-methods nicely if many sample paths have to be calculated for a well-understood parameter regime.

To state both schemes consider $t \in [0, T]$ and define $(\Delta t) := T/K$ for some fixed $K \in \mathbb{N}$. Denote the numerical solution by $U^k \approx U(k(\Delta t))$ where $k \in \{0, 1, 2, \dots, K\}$ and let $(\Delta B^k) = B((k + 1)(\Delta t)) - B(k(\Delta t))$ denote a vector of $\mathcal{N}(0, \Delta t)$ normally distributed independent increments used at the k -th time step. The explicit Euler-Maruyama method is given by

$$U_j^{k+1} = U_j^k + \Delta t F_j(U^k) + G_{jj}(U^k) (\Delta B^k)_j \quad (15)$$

for each component $j \in \{1, 2, \dots, N\}$. The explicit Milstein scheme for (14) - with diagonal noise matrix G - is given by [42, p.348,(3.12)]

$$U_j^{k+1} = U_j^k + \Delta t F_j(U^k) + G_{jj}(U^k) (\Delta B^k)_j + \frac{1}{2} G_{jj}(U^k) \frac{\partial G_{jj}}{\partial U_j}(U^k) [(\Delta B^k)_j^2 - \Delta t]. \quad (16)$$

For non-diagonal noise satisfying a suitable commutativity condition the scheme is still quite simple [42,

p.348,(3.16)] while for more general cases one has to be careful [38]. The implicit version of the Milstein scheme for our problem is [42, p.400]

$$U_j^{k+1} = U_j^k + \Delta t F_j(U^{k+1}) + G_{jj}(\square) (\Delta B^k)_j + \frac{1}{2} G_{jj}(\square) \frac{\partial G_{jj}}{\partial U_j}(\square) [(\Delta B^k)_j^2 - \Delta t] \quad (17)$$

where we have the choice to make the scheme fully-implicit with $\square = U^{k+1}$ or semi-implicit with $\square = U^k$. Since the deterministic drift term F causes the stability problems if $D(\Delta t) > (\Delta x)^2$ [24, p.64,67] it makes sense to chose the semi-implicit version. The algebraic problem to solve for U^{k+1} in (17) can be solved using standard techniques such as Newton's method.

It should be noted that the convergence and error estimate of the numerical scheme do not immediately yield error estimates for quantitative properties or scaling laws of traveling waves for the FKPP equation. For example, it has been demonstrated [18, p.71] that for pulled fronts of a discretized deterministic FKPP ($D = 1 = \mu$) the speed given to leading-order by

$$c^* = 2 - 2(\Delta t) + \frac{1}{12}(\Delta x)^2 + \dots \quad (18)$$

A similar effect is expected for the stochastic FKPP equation and properties such as the diffusion properties of the wave speed. Therefore, we have to view numerical scaling laws as approximations which carry some information about the discretization step sizes Δx and Δt . To minimize this effect, the formula (18), the stability requirement $\Delta t < (\Delta x)^2$ and the goal to minimize computation time indicate that we should choose Δt only slightly smaller than $(\Delta x)^2$.

We are not interested in computing the exact wave speed, only its trend under parameter variation will be relevant here. A simple method to compute an upper bound \hat{c} on the wave speed for the initial condition $u(0, 0) = 1$ and $u(x, 0) = 0$ for a stochastic wave is to collect the set of points $(j \Delta x, k \Delta t)$ such that $u(j \Delta x, k \Delta t)$ is less and $u((j-1) \Delta x, k \Delta t)$ is bigger than a threshold (usually we pick the threshold as 0.05). For each point one computes the estimate $c \approx \Delta x / \Delta t$ and obtains \hat{c} as the maximum.

6 Linear Multiplicative Noise

The first stochastic version of the FKPP equation we consider was studied by Elworthy, Zhao and Gaines [19, 24] and is given by

$$\frac{\partial u}{\partial t} = \frac{\mu^2}{2} \frac{\partial^2 u}{\partial x^2} + \frac{1}{\mu^2} u(1-u) + \hat{\epsilon} u \dot{B} \quad (19)$$

with one-dimensional time-dependent white noise \dot{B} , a small parameter $0 < \mu \ll 1$ and noise strength $\hat{\epsilon} > 0$. The multiplicative noise can be motivated e.g. by the interaction of a population u with the environment [78] or by parameter noise in the deterministic part [68, p.8] such as a fluctuating growth rate [83]. A multiplicative noise term of the form $g(u) = u$ has also been used in a model for plankton spreading [52, eq.(4b)]. For further mathematical background on SPDEs of the form (19) we refer to Section 4.

It is proven in [19] that there are three major regimes for (19) depending upon the noise strength parameter $\hat{\epsilon}$. For some $\kappa = \mathcal{O}(1)$ as $\mu \rightarrow 0$, the cases $\hat{\epsilon} \sim \kappa/\mu^2$, $\hat{\epsilon} \sim \kappa/\mu$ and $\hat{\epsilon} \sim \kappa$ are identified as the strong, mild and weak noise regimes respectively. Elworthy, Zhao and Gaines prove and numerically demonstrate that for weak noise the wave propagation of the pulled front is basically unaffected while the wave fails to propagate in the strong noise regime [19, Thms 8.1-8.3]. In the mild noise regime the wave speed is decreased as $\sqrt{2 - \kappa}$ [24, p.65]. It is important to note that the spontaneous collapse of newly-introduced alien populations, which can occur in a strong noise regime, has been considered from an applied perspective in [76].

Using the scaling law of Brownian motion and the transformation

$$x \mapsto \frac{x\mu^2}{\sqrt{2}}, \quad t \mapsto t\mu^2, \quad \epsilon := \mu\hat{\epsilon},$$

as discussed in Section 3, in the SPDE (19) yields the more familiar form of the FKPP equation

$$\frac{\partial u}{\partial t} = \frac{\partial^2 u}{\partial x^2} + u(1-u) + \epsilon u \dot{B}. \quad (20)$$

This gives the quite natural view that $\epsilon \gg 1$, $\epsilon \sim 1$ and $\epsilon \ll 1$ are the strong, mild and weak noise regimes. Figure 1 shows typical solutions for the three regimes; for details on the numerical methods see Section 5. The initial condition is taken as the introduction of a species at a particular fixed location so that

$$u(x, t = 0) = \begin{cases} 1 & \text{if } x = 0, \\ 0 & \text{otherwise.} \end{cases} \quad (21)$$

It is understood that the numerical initial condition is obtained by choosing a mesh having a mesh point $x = 0$ with $u(0, 0) = 1$.

Now consider the situation of the 'ecological observer' who can only measure the invasion wave at one particular point in space. Based on the results by

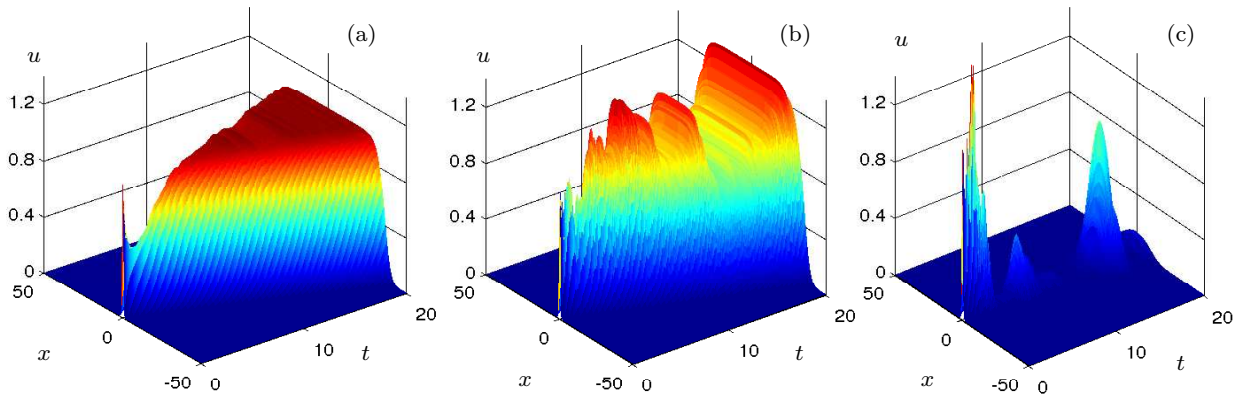


Fig. 1 Simulation of (20) using the implicit Milstein scheme (17) with parameters $K = 100$, $T = 20$, $N = 10^3$ on the interval $[-50, 50]$ with Neumann boundary conditions and initial condition $u(x, 0) = 1$ if $x = 0$ and $u(x, 0) = 0$ otherwise. (a) $\epsilon = 0.02$, (b) $\epsilon = 0.3$ and (c) $\epsilon = 1.2$.

Elworthy, Zhao and Gaines [19,24] on propagation failure of the wave with increasing noise strength it is intuitive that the local statistics recorded at a fixed point carry information about the traveling front.

For convenience we pick the point as $x = 0$. Consider a single sample path $u(0, t)$. Let T denote the final time and consider the two basic statistics

$$\bar{u} = \frac{1}{T-t_0} \int_{t_0}^T u(0, t) dt,$$

$$\Sigma = \left[\frac{1}{T-t_0} \int_{t_0}^T (u(0, t) - \bar{u})^2 dt \right]^{1/2}.$$

Figure 2 shows an average of \bar{u} over 200 sample paths which we denote by \bar{U} . From the results it is becoming clear, once one compares the \bar{U} plot with the \hat{c} plot, that a decreasing mean population size does provide the expected early-warning sign for a decreased invasion front speed. We also simulated the same case shown in Figure 2 for space-time white noise \dot{W} in (20). The results are qualitatively similar with a slight quantitative shift towards faster waves at comparable noise strength.

In both cases a relevant new result is that also the local fluctuations captured by the variance show a quite interesting behavior. Consider the scenario where the actual carrying capacity for the population is unknown. In this case, the population level \bar{u} is insufficient to determine how far we are from propagation failure of the wave. Naively, one may interpret small population fluctuations as an indicator for a fast propagating wave but Figure 2 shows that it could equally well be a very slow propagating wave for a low population level. Hence one has to increase or decrease the noise strength to probe to which part of Figure 2 the observations match.

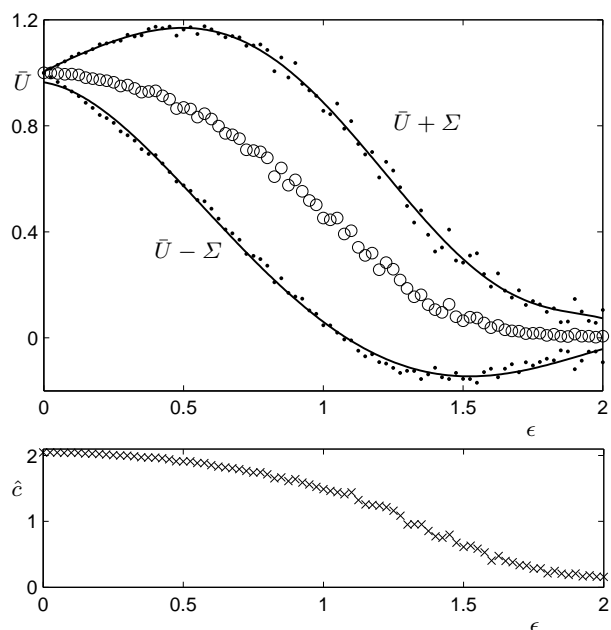


Fig. 2 Dependence of the time average \bar{U} and the wave speed c on the noise strength ϵ averaged over 200 sample paths. The SPDE (20) has been numerically solved (using Euler-Maruyama (15)) with $K = 100$, $T = 20$, $N = 10^3$ on the interval $[-50, 50]$ with Neumann boundary conditions and initial condition $u(x, 0) = 1$ if $x = 0$ and $u(x, 0) = 0$ otherwise. The top part shows \bar{U} (circles) which has been calculated as the mean of the time series $u(0, t)$ recorded by an ecological observer at the origin for $t \in [10, 20]$. The dots indicate ± 1 standard deviation Σ for the time series; the curves are associated interpolations forming a confidence neighborhood. The bottom part of the figure shows an (upper bound) estimate for the wave speed.

7 Nonlinear Multiplicative Noise

As pointed out at the beginning of Section 6, the noise terms $\epsilon u \dot{B}$ and $\epsilon u \dot{W}$ could be interpreted as

parametric or environmental noise. Another possible source of noise is 'individual-based' or 'finite-system-size' which we shall focus on in this section. Müller and Tribe showed in [57] that the SPDE

$$\frac{\partial u}{\partial t} = \frac{1}{6} \frac{\partial^2 u}{\partial x^2} + \mu u(1-u) + \sqrt{2u} \dot{W} \quad (22)$$

arises as a limit of a contact process on a lattice originally studied in [5] as a model for long-range offspring displacement; traveling wave solutions to (22) exist for suitable parameter values [80]. However, Müller and Tribe also studied the behavior of (22) with a scaled noise term $\sqrt{u} \dot{W}$ varying the parameter μ and proved [56, Thm 1] that there exists a critical value μ_c , independent of $u(x, 0)$, such that

$$\begin{aligned} \mathbb{P}(u(x, t) \text{ survives}) &= 0 \text{ if } \mu < \mu_c, \\ \mathbb{P}(u(x, t) \text{ survives}) &= 1 \text{ if } \mu > \mu_c. \end{aligned} \quad (23)$$

Hence propagation failure of waves can occur like in the situation with noise term $u\dot{W}$. Using the mapping $t \mapsto t/\mu$, $x \mapsto x/\sqrt{6\mu}$, a standard scaling law result [56, Lem 2.1.1] and the definition $\epsilon := \sqrt{2}(6/\mu)^{1/4}$ transform (22) to

$$\frac{\partial u}{\partial t} = \frac{\partial^2 u}{\partial x^2} + \mu u(1-u) + \epsilon \sqrt{u} \dot{W}. \quad (24)$$

Figure 3 shows the dependence of the population level, its fluctuations and the wave speed on the parameter ϵ . The results are very similar to Figure 2 with propagation failure for higher noise level as expected from (23). In particular, the conclusions from Section 6 about inferring wave propagation properties from local data still apply. One may conjecture that the conclusions might apply to even more general versions of the FKPP equation with a noise term $\epsilon g(u)\dot{W}$ (or $\epsilon g(u)\dot{B}$) as long as $g(0) = 0$.

However, the SPDEs (20) and (24) have noise terms that increase monotonically with the population level. This may not be realistic in all situations as one expects the noise to change as u approaches the carrying capacity. This is one motivation to study the SPDE

$$\frac{\partial u}{\partial t} = \frac{\partial^2 u}{\partial x^2} + \mu u(1-u) + \epsilon \sqrt{u(1-u)} \dot{W}. \quad (25)$$

This model was studied by several groups. In [55] it was proved for sufficiently small noise that compactly supported initial data remain within a time-dependent interval and that a well-defined front as well as an asymptotic wave speed exist; interestingly, the shape and asymptotic form of waves has been

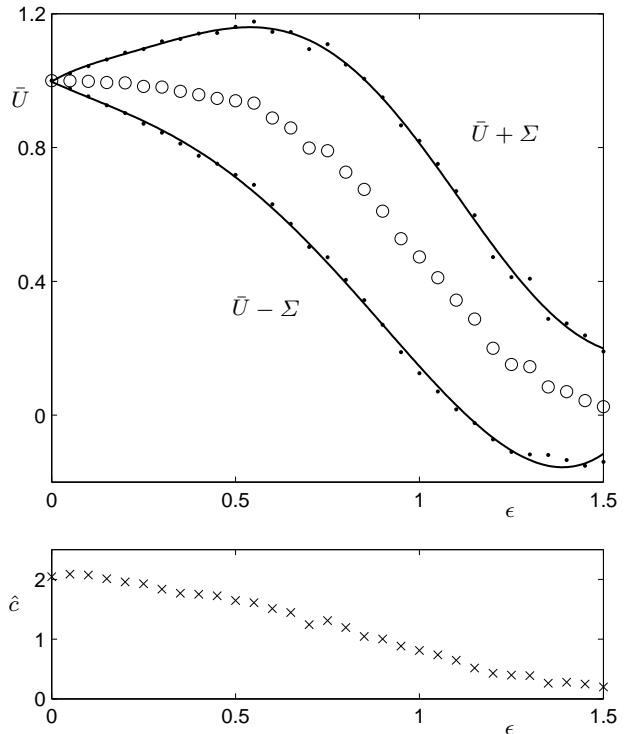


Fig. 3 Dependence of the time average \bar{U} and the wave speed on the noise strength ϵ for (24). Parameter values are as for Figure 2.

of interest by an independent group for a discrete stochastic model [50].

Detailed numerical studies of the wave speed for (25) have been carried out [62, 8] focusing on the small noise regime and the fluctuation properties of the front. Due to the special structure of the FKPP equation one may also exploit a duality argument of (25) to a particle system [15, 75]. Doering, Müller and Smereka conjecture [15, eq (55)] from the duality relation that the asymptotic wave speed in the strong noise regime is given by $c \sim 2/\epsilon^2$ as $\epsilon \rightarrow \infty$. Although it is unclear whether this conjecture is correct it is evident from numerical simulations [15, Fig 2] that the wave speed decreases upon increasing the noise.

Figure 4 shows the mean, standard deviation and wave speed calculated for (25). There are some minor differences between this case and $g(u) = u$ and $g(u) = \sqrt{u}$ shown in Figures 2 and 3. There is a larger plateau for small noise and it takes larger noise strengths to reach the vicinity of propagation failure. However, the main warning-signs from local data still remain as it is still possible to conclude from large population levels and low fluctuations a

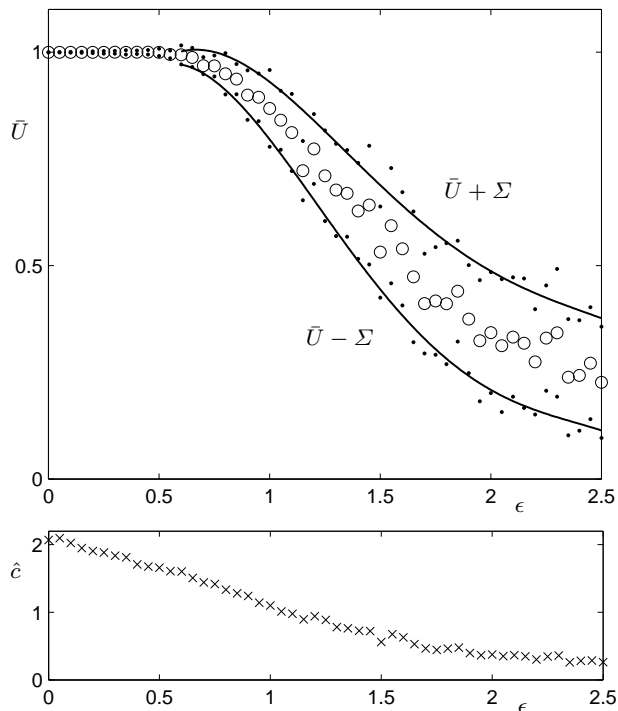


Fig. 4 Dependence of the time average \bar{U} and the wave speed on the noise strength ϵ for (25). Parameter values are as for Figure 2 except for the slightly smaller time-step size $N = 3 \cdot 10^3$.

fast wave while increasing fluctuations lead to slower speeds and low population levels with smaller fluctuations indicate closeness to propagation failure.

Another different form of the noise term given by $g(u) = u(1 - u)$ was considered in [68, eq (39)-(41)] but we shall not consider it here as the results are similar.

In summary, one should always measure the closeness to carrying capacity and the size of the fluctuations (standard deviation, variance). If system parameters change slowly one may determine from Figures 2-4 whether the distance to propagation failure has increased or decreased.

8 Transitions for the Allee Effect

Although propagation failure is extremely interesting from the viewpoint of critical transitions, it is certainly not the only invasion wave phenomenon where local early-warning signs are desirable. As already discussed in Section 3 there can also be pushed fronts if the nonlinearity $f(u)$ is chosen differently. A reasonable prototypical model to study is the fol-

lowing SPDE

$$\frac{\partial u}{\partial t} = \frac{\partial^2 u}{\partial x^2} + u(1 - u)(u - \mu) + \epsilon g(u) \dot{W} \quad (26)$$

which has been considered in [68]. The nonlinearity $f(u) = u(1 - u)(u + \mu)$ may obviously arise due to an Allee effect in the context of ecology but it is also commonly used in other areas of mathematical biology, e.g. in neuroscience (26) would be referred to as Nagumo's equation [60]. We briefly recall some results about the deterministic PDE ($\epsilon = 0$) described in [65]. For $\mu \in [-1/2, 1/2]$ there exists a closed-form wave

$$u(x, t) = u(x - ct) = u(\xi) = \frac{1}{1 + e^{\frac{1}{\sqrt{2}}(\xi - \xi^-)}}$$

for an arbitrary phase $\xi^- > 0$ and propagation speed

$$c = \frac{1}{\sqrt{2}} - \sqrt{2}\mu. \quad (27)$$

There are three interesting special points. For $\mu = 1/2$ the front speed vanishes and the front reverses direction if $\mu > 1/2$. The regime for $\mu \in (0, 1/2)$ is called bistable and changes to a pushed front at $\mu = 0$; see [65, Sec 1] and references therein for details. The pushed front regime applies for $\mu \in (-1/2, 0)$ and at $\mu = -1/2$ there is a pushed-to-pulled front transition [68, Sec V]. The wave speed for the pulled front is $c^* = 2\sqrt{-\mu}$ [64, Sec 3.3][81, p.38-42]. Therefore, it is interesting to try to find early-warning signs for approaching the three special points $\mu = -1/2, 0, 1/2$ cases. The front reversal case $\mu = 1/2$ is clearly important as a direction change for an invasion front could be regarded as a critical transition but the other two cases could be of interest as well.

For the SPDE (26) we shall choose the simple multiplicative noise $g(u) = u$. We consider the pushed-to-pulled transition first and try to apply our approach from Sections 6-7. Figure 5 shows the analog of the top parts of Figures 2-4. We observe that it is impossible to detect a trend or infer the speed of the wave. Hence, for the pushed-to-pulled transition with space-time white noise the classical variance-based early-warning signs cannot be applied for local data perturbed by a fixed noise level and observed at the center of the wave. Therefore, one should also think of new early-warning sign techniques in the context of wave propagation.

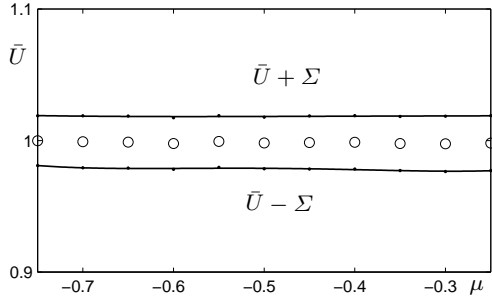


Fig. 5 Dependence of the time average \bar{U} on the noise strength ϵ averaged over 200 sample paths. The SPDE (26) for $g(u) = u$ has been numerically solved (using Euler-Maruyama (15)) with $K = 100$, $T = 15$, $N = 10^3$ on the interval $[-50, 50]$ with Neumann boundary conditions and initial condition $u(x, 0) = 1$ if $x \in [-1, 1]$ and $u(x, 0) = 0$ otherwise. \bar{U} (circles) has been calculated as the mean of the time series $u(0, t)$ recorded by an ecological observer at the origin for $t \in [7.5, 15]$. The dots indicate ± 1 standard deviation Σ for the time series; the curves are associated interpolations forming a confidence neighborhood.

Note carefully that we always used in our computations in Figures 2-5 the regime for $u(0, t)$ when the wave is already fully formed with $t \in [T_0, T]$ for some $T_0 \gg 1$. However, the transient regime starting from the localized initial condition may also contain important information. Figure 6 shows three numerical simulations for $\mu = -0.3, 0.2, 0.4$.

The computation suggests that the initial transient spreading of the wave $u(0, t)$ for $t \in [0, T_0]$ is interesting. A simple measure to consider is

$$u_m := \min_{t \in [0, T_0]} \{u(0, t) : \text{for a given } u(x, 0)\}. \quad (28)$$

Clearly, the result depends upon the choice of T_0 and the initial condition $u(x, 0)$. However, if both are fixed then we may compare the results. Figure 7(a) shows the results for a parametric study of $\mu \in [-0.75, 0.5]$. The insets (b)-(c) show a finer mesh resolution near the pushed-to-pulled transition at $\mu = -1/2$ and near propagation failure which is slightly shifted from the theoretical value at $\mu = 1/2$ as the small finite-width initial condition and the noise both seem to contribute to reach the absorbing state $u \equiv 0$ for parameter values μ smaller than $1/2$. In fact, due to these effects, the transition is more drastic than the formula (27) predicts.

From Figure 7(b) it is apparent that the pushed-to-pulled transition is probably unpredictable from local data collected at $x = 0$. Since the wave speed transition is continuous one should probably not classify the pushed-to-pulled transition as a 'critical transition'. Therefore, it is not crucial to predict it but

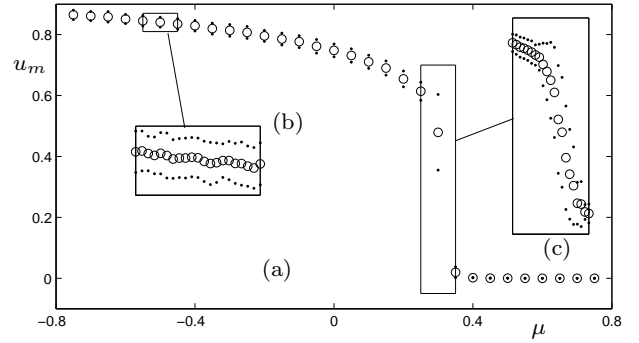


Fig. 7 (a) Dependence of the minimum u_m defined in 28 on μ with $T_0 = 10$, averaged over 200 sample paths. The SPDE (26) for $g(u) = u$ has been numerically solved (using Euler-Maruyama (15)) with $K = 100$, $T = 20$, $\epsilon = 0.05$, $N = 10^3$ on the interval $[-50, 50]$ with Neumann boundary conditions and initial condition $u(x, 0) = 1$ if $x \in [-1, 1]$ and $u(x, 0) = 0$ otherwise. The circles indicate u_m and the dots ± 1 standard deviation Σ calculated from the sample paths. (b) Zoom near the theoretical pushed-to-pulled transition at $\mu = 1/2$. (c) Zoom near propagation failure transition.

the result shows the limitation of the ecological observer at $x = 0$. The same conclusion applies to the change from the pushed to the bistable regime at $\mu = 0$. For the propagation failure scenario Figure 7(c) shows a scaling law for the decrease of u_m and a slightly increasing variance may help us to anticipate the upcoming critical transition. This should not be surprising since we already considered similar propagation failure cases in Sections 6-7. The difference is that we used a completely different indicator in Figure 7(c).

As for the classical FKPP equation one should remark for the Allee effect situation that different noise terms certainly do make sense, e.g. $g(u) = u(1 - u)$ considered in [2, eq.(2)]. Based on the observations for varying the noise terms for the classical FKPP equation, and obtaining similar results for several choices, we shall not consider these generalizations for (26).

9 Noncompact Initial Invasions

Based on the results in Section 8 we have observed that the initial transient regime, starting from a localized invasion wave, can be useful. It remains to consider the case when the initial condition is not localized. In particular, we consider the FKPP equation

$$\frac{\partial u}{\partial t} = \frac{\partial^2 u}{\partial x^2} + u(1 - u) + \epsilon u \dot{W}. \quad (29)$$

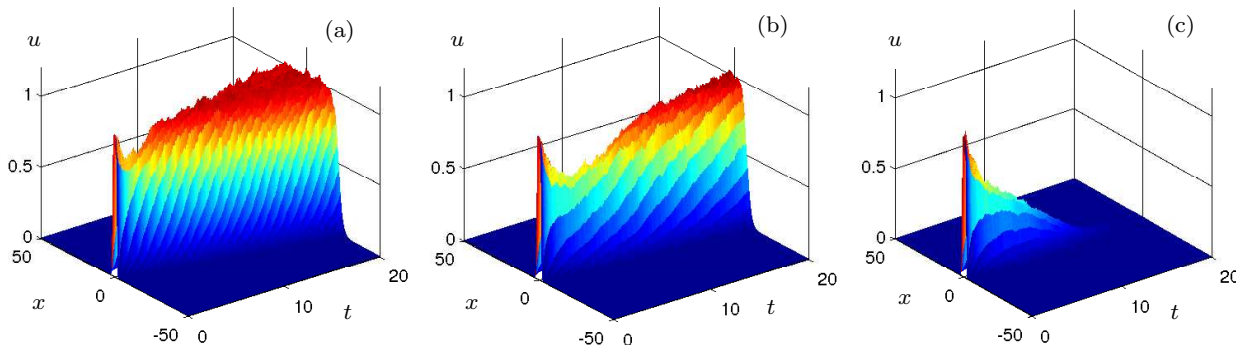


Fig. 6 Simulation of (26) for $g(u) = u$ using the implicit Milstein scheme (17) with parameters $K = 100$, $T = 20$, $N = 2 \cdot 10^3$ on the interval $[-50, 50]$ with Neumann boundary conditions and initial condition $u(x, 0) = 1$ if $x \in [-1, 1]$ and $u(x, 0) = 0$ otherwise. (a) $\mu = -0.3$, (b) $\mu = 0.2$ and (c) $\mu = 0.4$.

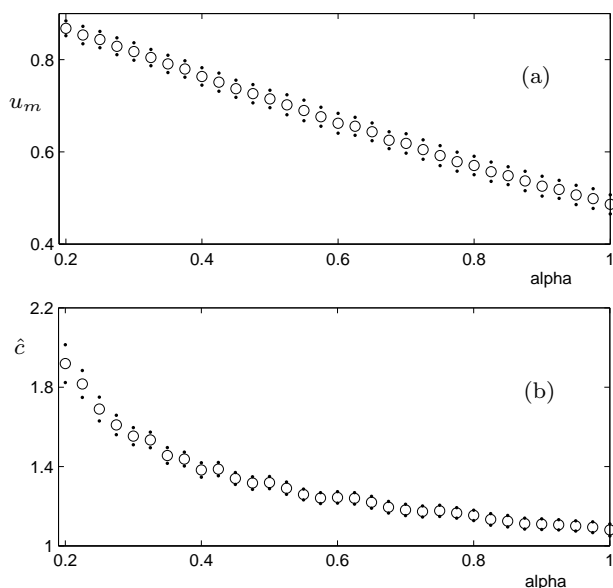


Fig. 8 Dependence of the minimum u_m defined in 28 on α for (29)-(30); average over 200 sample paths. The parameters for the numerical simulation (using Euler-Maruyama (15)) on the interval $[-50, 50]$ with Neumann boundary conditions are $K = 150$, $T = 10$, $\epsilon = 0.05$ and $N = 500$. (a) The circles indicate u_m and the dots ± 1 standard deviation calculated from the sample paths. (b) Wave speed \hat{c} (circles) and associated ± 1 standard deviation (dots).

with initial condition

$$u(x, 0) = e^{-\alpha|x|}, \quad \text{for } \alpha > 0. \quad (30)$$

Recall from Section 3 that the wave speed scales as $c(\alpha) = \mathcal{O}(1/\alpha)$ for $\alpha \rightarrow 0$.

Figure 8(a) shows the dependence of the initial transient observed at $x = 0$ on the complete initial data. Therefore, small minimum values indicate comparatively slower waves and no response to the initial condition ($u_m \approx 1$) signals a very fast wave.

Figure 8(b) shows an upper bound to the wave speed and raises the interesting question whether we should, or should not, view a blow-up point for the wave speed as a critical transition.

There are two main conclusions from the results for (29)-(30) and from Section 8. Firstly, one definitely should try to measure an invasion wave immediately once the first occurrence of a new population in a new environment has been observed. Secondly, knowing the basic structure of the initial condition can be crucial for prediction, e.g. in Figure 7 $0 \ll u_m < 1$ still indicates a well-defined asymptotic wave speed in the pushed regime while for Figure 8 the condition $0 \ll u_m < 1$ indicates closeness to a wave speed blow-up point. Hence, it is crucial to know, on a qualitative level, whether the initial invasion is really localized or whether it really consists of a full front.

10 Outlook

Since early-warning signs and stochastic scaling laws for noisy traveling waves are still a relatively new direction, we have only been able to cover a few aspects here. Many open problems arose which we summarize here.

The restrictions to one spatial dimension $x \in \mathbb{R}$ and one population component u have to be removed in the future. There are many interesting cases e.g. multi-component systems such as reaction-diffusion models with predation [61], FKPP-type plankton dynamics [6] or Nagumo (Allee effect)-type equations [27]. Multiple spatial dimensions can lead to more complicated bifurcation structures [40]. One may also remove all restrictions which can generate interesting life-death transitions for multi-component, 2D and

3D systems [58]. Another highly relevant generalization are heterogeneous [69] and random [85] environments. Furthermore, the structure of the FKPP equation may be too restrictive which suggests to add transport/advection terms and active boundaries in which case discontinuous wave speed transitions have been reported [11]. Also the assumption of time-white or space-time-white noise is too restrictive and one should extend the view to spatially-colored noise [25] and trace-class covariance operators. Another issue that looked interesting is the relevance of fluctuations ('front diffusion') [1,67] for early-warning signs.

In all cases, our main driving question in this paper seems to be open: How much information do local statistics of an SPDE, collected at one (or multiple) locations, carry about the speed and bifurcations of traveling waves? It seems plausible to obtain basic answers to these questions using numerical simulations. To develop a mathematical theory for quantitative scaling laws of SPDEs and their application to critical transitions is expected to be a challenging problem for a long time.

Acknowledgements: I would like to thank the European Commission (EC/REA) for support by a Marie-Curie International Re-integration Grant.

References

1. J. Armero, J. Casademunt, L. Ramirez-Piscina, and J.M. Sancho. Ballistic and diffusive corrections to front propagation in the presence of multiplicative noise. *Phys. Rev. E*, 58(5):5494–5500, 1998.
2. J. Armero, J.M. Sancho, J. Casademunt, A.M. Lacasta, L. Ramirez-Piscina, and F. Sagués. External fluctuations in front propagation. *Phys. Rev. Lett.*, 76(17):3045–3048, 1996.
3. L. Arnold. *Stochastic Differential Equations: Theory and Applications*. Wiley, 1974.
4. R.D. Benguria and M.C. Depassier. Speed of fronts of the reaction-diffusion equation. *Phys. Rev. Lett.*, 77(6):1171–1173, 1996.
5. M. Bramson, R. Durrett, and G. Swindle. Statistical mechanics of crabgrass. *Ann. Probab.*, 17:444–481, 1989.
6. J. Brindley, V.H. Biktashev, and M.A. Tsyganov. Invasion waves in populations with excitable dynamics. *Biological Invasions*, 7:807–816, 2005.
7. E. Brunet and B. Derrida. Shift in the velocity front due to a cutoff. *Phys. Rev. E*, 56(3):2597–2604, 1997.
8. E. Brunet, B. Derrida, A.H. Mueller, and S. Munier. Phenomenological theory giving full statistics of the position of fluctuating fronts. *Phys. Rev. E*, 73:(056126), 2006.
9. S.R. Carpenter, J.J. Cole, M.L. Pace, R. Batt, W.A. Brock, T. Cline, J. Coloso, J.R. Hodgson, J.F. Kitchell, D.A. Seekell, L. Smith, and B. Weidel. Early warning signs of regime shifts: a whole-ecosystem experiment. *Science*, 332:1079–1082, 2011.
10. P.-L. Chow. *Stochastic Partial Differential Equations*. Chapman & Hall / CRC, 2007.
11. A. Costa, R.A. Blythe, and M.R. Evans. Discontinuous transition in a boundary driven contact process. *J. Stat. Mech. Theor. Exp.*, 2010(9):(P09008), 2010.
12. M.C. Cross and P.C. Hohenberg. Pattern formation outside of equilibrium. *Rev. Mod. Phys.*, 65(3):851–1112, 1993.
13. V. Dakos, M. Kéfi, M. Rietkerk, E.H. van Nes, and M. Scheffer. Slowing down in spatially patterned systems at the brink of collapse. *Am. Nat.*, 177(6):153–166, 2011.
14. V. Dakos, E.H. van Nes, R. Donangelo, H. Fort, and M. Scheffer. Spatial correlation as leading indicator of catastrophic shifts. *Theor. Ecol.*, 3(3):163–174, 2009.
15. C.R. Doering, C. Mueller, and P. Smereka. Interacting particles, the stochastic Fisher–Kolmogorov–Petrovsky–Piscounov equation, and duality. *Physica A*, 325:243–259, 2003.
16. J.M. Drake and B.D. Griffen. Early warning signals of extinction in deteriorating environments. *Nature*, 467:456–459, 2010.
17. R. Durrett. *Probability: Theory and Examples - 4th edition*. CUP, 2010.
18. U. Ebert and W. van Saarloos. Front propagation into unstable states: universal algebraic convergence towards uniformly translating pulled fronts. *Physica D*, 146:1–99, 2000.
19. K.D. Elworthy, H.Z. Zhao, and J.G. Gaines. The propagation of travelling waves for stochastic generalized KPP equations. *Mathl. Comput. Modelling*, 20(4):131–166, 1994.
20. W.F. Fagan, M.A. Lewis, M.G. Neubert, and P. van den Driessche. Invasion theory and biological control. *Ecol. Lett.*, 5:148–157, 2002.
21. J.A.N. Filipe, W. Otten, G.J. Gibson, and C.A. Gilligan. Inferring the dynamics of a spatial epidemic from time-series data. *Bull. Math. Biol.*, 66:379–391, 2004.
22. R.A. Fisher. The wave of advance of advantageous genes. *Ann. Eugenics*, 7:353–369, 1937.
23. F. Flandoli. Stochastic flows for nonlinear second-order parabolic SPDE. *Ann. Probab.*, 24(2):547–558, 1996.
24. J.G. Gaines. Numerical experiments with S(P)DEs. In A. Etheridge, editor, *Stochastic Partial Differential Equations*, volume 216 of *LMS Lecture Note Series*, pages 55–71. CUP, 1995.
25. J. Garcia-Ojalvo and J. Sancho. *Noise in Spatially Extended Systems*. Springer, 1999.
26. I. Golding, Y. Kozlovsky, I. Cohen, and E. Ben-Jacob. Studies of bacterial branching growth using reaction-diffusion models for colonial development. *Physica A*, 260:510–554, 1998.
27. J. Guckenheimer and C. Kuehn. Homoclinic orbits of the FitzHugh-Nagumo equation: Bifurcations in the full system. *SIAM J. Appl. Dyn. Syst.*, 9:138–153, 2010.
28. I. Gyöngy. Lattice approximations for stochastic quasi-linear parabolic partial differential equations driven by space-time white noise I. *Potential Anal.*, 9:1–25, 1998.

29. M. Hairer. *An Introduction to Stochastic Partial Differential Equations*. Lecture Notes, 2009. <http://www.hairer.org/notes/SPDEs.pdf>.
30. F. Hamel and N. Nadirashvili. Travelling fronts and entire solutions of the Fisher-KPP equation in \mathbb{R}^N . *Arch. Ration. Mech. Anal.*, 157:91–163, 2001.
31. A. Hastings, K. Cuddington, K.F. Davies, C.J. Dugaw, S. Elmendorf, A. Freestone, S. Harrison, M. Holland, J. Lambrinos, U. Malvadkar, B.A. Melbourne, and K. Moore. The spatial spread of invasions: new developments in theory and evidence. *Ecol. Lett.*, 8:91–101, 2005.
32. D.J. Highham. An algorithmic introduction to numerical simulation of stochastic differential equations. *SIAM Review*, 43(3):525–546, 2001.
33. F.M. Hilker, M.A. Lewis, H. Seno, M. Langlais, and H. Malchow. Pathogens can slow down or reverse invasion fronts of their hosts. *Biological Invasions*, 7:817–832, 2005.
34. M. Hirota, M. Holmgren, E.H. van Nes, and M. Scheffer. Global resilience of tropical forest and savanna to critical transitions. *Science*, 334:232–235, 2011.
35. D.A. Holway. Factors governing rate invasion: a natural experiment using Argentine ants. *Oecologia*, 115:206–212, 1998.
36. R. Hoyle. *Pattern Formation: An introduction to methods*. Cambridge University Press, 2006.
37. A. Jentzen and P.E. Kloeden. The numerical approximation of stochastic partial differential equations. *Milan J. Math.*, 77:205–244, 2009.
38. A. Jentzen and M. Röckner. A Milstein scheme for SPDEs. *arXiv:1001.2751v4*, pages 1–37, 2012.
39. G. Jetschke. On the equivalence of different approaches to stochastic partial differential equations. *Math. Nachr.*, 128:315–329, 1986.
40. P.M. Jordan and A. Puri. Qualitative results for solutions of the steady Fisher-KPP equation. *Appl. Math. Lett.*, 15:239–250, 2002.
41. S. Kéfi, M. Rietkerk, C.L. Alados, Y. Peyo, V.P. Papanastasis, A. ElAich, and P.C. de Ruiter. Spatial vegetation patterns and imminent desertification in mediterranean arid ecosystems. *Nature*, 449:213–217, 2007.
42. P.E. Kloeden and E. Platen. *Numerical Solution of Stochastic Differential Equations*. Springer, 2010.
43. A. Kolmogorov, I. Petrovskii, and N. Piscounov. A study of the diffusion equation with increase in the amount of substance, and its application to a biological problem. In V.M. Tikhomirov, editor, *Selected Works of A. N. Kolmogorov I*, pages 248–270. Kluwer, 1991. Translated by V. M. Volosov from Bull. Moscow Univ., Math. Mech. 1, 1–25, 1937.
44. A. Kölzsch and B. Blasius. Indications of marine bioinvasion from network theory. An analysis of the global cargo ship network. *Euro. Phys. J. B*, 84:601–612, 2011.
45. C. Kuehn. A mathematical framework for critical transitions: bifurcations, fast-slow systems and stochastic dynamics. *Physica D*, 240(12):1020–1035, 2011.
46. C. Kuehn. A mathematical framework for critical transitions: normal forms, variance and applications. *J. Nonl. Sci.*, pages 1–56, 2012. accepted.
47. Yu.A. Kuznetsov. *Elements of Applied Bifurcation Theory*. Springer, New York, NY, 3rd edition, 2004.
48. A. Lemarchand, A. Lesne, and M. Mareschal. Langevin approach to a chemical wave front: selection of the propagation velocity in the presence of internal noise. *Phys. Rev. E*, 51(5):4457–4465, 1995.
49. M. Lewis. Spread rate for a nonlinear stochastic invasion. *J. Math. Biol.*, 41:430–454, 2000.
50. M. Lewis and S. Pacala. Modeling and analysis of stochastic invasion processes. *J. Math. Biol.*, 41:387–429, 2000.
51. W.M. Lonsdale. Rates of spread of an invading species: mimosa pigra in Northern Australia. *J. Ecol.*, 81:513–521, 1993.
52. H. Malchow, F.M. Hilker, S.V. Petrovskii, and K. Brauer. Oscillations and waves in a virally infected plankton system. Part I: The lysogenic stage. *Ecol. Complexity*, 1(3):211–233, 2004.
53. J.A.J. Metz, D. Mollison, and F. van den Bosch. The dynamics of invasion waves. In U. Dieckmann, R. Law, and J.A.J. Metz, editors, *The Geometry of Ecological Interactions: Simplifying Spatial Complexity*, pages 482–512. CUP, 2000.
54. M. Mimura, H. Sakaguchi, and M. Matsushita. Reaction-diffusion modelling of bacterial colony patterns. *Physica A*, 282:283–303, 2000.
55. C. Mueller and R.B. Sowers. Random travelling waves for the KPP equation with noise. *J. Funct. Anal.*, 128(2):439–498, 1995.
56. C. Mueller and R. Tribe. A phase transition for a stochastic PDE related to the contact process. *Probab. Theory Relat. Fields*, 100:131–156, 1994.
57. C. Mueller and R. Tribe. Stochastic PDEs arising from the long range contact and long range voter processes. *Probab. Theory Relat. Fields*, 102:519–545, 1995.
58. C. Mueller and R. Tribe. A phase diagram for a stochastic reaction diffusion system. *Probab. Theory Relat. Fields*, 149:561–637, 2011.
59. J.D. Murray. *Mathematical Biology I: An Introduction*. Springer, 3rd edition, 2002.
60. J. Nagumo, S. Arimoto, and S. Yoshizawa. An active pulse transmission line simulating nerve axon. *Proc. IRE*, 50:2061–2070, 1962.
61. M.R. Owen and M.A. Lewis. How predation can slow, stop or reverse a prey invasion. *Bull. Math. Biol.*, 63:655–684, 2001.
62. L. Pechenik and H. Levine. Interfacial velocity corrections due to multiplicative noise. *Phys. Rev. E*, 59(4):3893–3900, 1999.
63. B.L. Phillips, G.P. Brown, J.K. Webb, and R. Shine. Invasion and the evolution of speed in toads. *Nature*, 439:803, 2006.
64. N. Popovic. A geometric classification of traveling front propagation in the Nagumo equation with cut-off. In *MURPHYS 2010: Proceedings of the International Workshop on Multi-Rate Processes and Hysteresis, Pecs, 2010*, volume 268 of *J. Phys. Conference Series*, page (012023), 2011.
65. N. Popovic. A geometric analysis of front propagation in an integrable Nagumo equation with a linear cut-off. *Physica D*, 241:1976–1984, 2012.
66. G. Da Prato and J. Zabczyk. *Stochastic Equations in Infinite Dimensions*. Cambridge University Press, 1992.
67. A. Rocco, J. Casademunt, U. Ebert, and W. van Saarloos. Diffusion coefficient of propagating fronts with multiplicative noise. *Phys. Rev. E*, 65:(012102), 2001.

68. A. Rocco, L. Ramirez-Piscina, and J. Casademunt. Kinematic reduction of reaction-diffusion fronts with multiplicative noise: derivation of stochastic sharp-interface equations. *Phys. Rev. E*, 65:(056116), 2002.
69. L. Roques and F. Hamel. Mathematical analysis of the optimal habitat configurations for species persistence. *Math. Biosci.*, 210:34–59, 2007.
70. L. Roques, F. Hamel, J. Fayard, B. Fady, and E.K. Klein. Recolonisation by diffusion can generate increasing rates of spread. *J. Theor. Biol.*, 77:205–212, 2010.
71. M. Scheffer, J. Bascompte, W.A. Brock, V. Brovkhin, S.R. Carpenter, V. Dakos, H. Held, E.H. van Nes, M. Rietkerk, and G. Sugihara. Early-warning signals for critical transitions. *Nature*, 461:53–59, 2009.
72. M. Scheffer, S. Carpenter, J.A. Foley, C. Folke, and B. Walker. Catastrophic shifts in ecosystems. *Nature*, 413:591–596, 2001.
73. M. Scheffer and S.R. Carpenter. Catastrophic regime shifts in ecosystems: linking theory to observation. *TRENDS in Ecol. and Evol.*, 18(12):648–656, 2003.
74. M. Scheffer and E.H. van Nes. Shallow lakes theory revisited: various alternative regimes driven by climate, nutrients, depth and lake size. *Hydrobiologia*, 584:455–466, 2007.
75. T. Shiga and K. Uchiyama. Stationary states and the stability of the stepping stone model involving mutation and selection. *Probab. Theory Related Fields*, 73:87–117, 1986.
76. D. Simberloff and L. Gibbons. Now you see them, now you dont! population crashes of established introduced species. *Biological Invasions*, 6:161–172, 2004.
77. J.G. Skellam. Random dispersal in theoretical populations. *Biometrika*, 38(1):196–218, 1951.
78. B. Spagnolo, A. Fiasconaro, and D. Valenti. Noise induced phenomena in Lotka-Volterra systems. *Fluct. Noise Lett.*, 3(2):177–185, 2003.
79. C.D. Thomas, E.J. Bodsworth, R.J. Wilson, A.D. Simmons, Z.G. Davies, M. Musche1, and L. Conradt. Ecological and evolutionary processes at expanding range margins. *Nature*, 411:577–581, 2001.
80. R. Tribe. A travelling wave solution to the Kolmogorov equation with noise. *Stochastics*, 56(3):317–340, 1996.
81. W. van Saarloos. Front propagation into unstable states. *Physics Reports*, 386:29–222, 2003.
82. A.J. Veraart, E.J. Faassen, V. Dakos, E.H. van Nes, M. Lurling, and M. Scheffer. Recovery rates reflect distance to a tipping point in a living system. *Nature*, 481:357–359, 2012.
83. J.M.G. Vilar and R.V. Solé. Effects of noise in symmetric two-species competition. *Phys. Rev. Lett.*, 80(18):4099–4102, 1998.
84. J.B. Walsh. An introduction to stochastic partial differential equations. In *École d’été de probabilités de Saint-Flour, XIV - 1984*, volume 1180 of *Lecture Notes in Math.*, pages 265–439. Springer, 1986.
85. J. Xin. *An Introduction to Fronts in Random Media*. Springer, 2009.